

# Speed and accuracy of olfactory discrimination in the rat

Naoshige Uchida & Zachary F Mainen

The sense of smell is typically thought of as a 'slow' sense, but the true temporal constraints on the accuracy of olfactory perception are not known. It has been proposed that animals make finer odor discriminations at the expense of additional processing time. To test this idea, we measured the relationship between the speed and accuracy of olfactory discrimination in rats. We found that speed of discrimination was independent of odor similarity, as measured by overlap of glomerular activity patterns. Even when pushed to psychophysical limits using mixtures of two odors, rats needed to take only one sniff (<200 ms at theta frequency) to make a decision of maximum accuracy. These results show that, for the purpose of odor quality discrimination, a fully refined olfactory sensory representation can emerge within a single sensorimotor or theta cycle, suggesting that each sniff can be considered a snapshot of the olfactory world.

The main olfactory system uses a large repertoire of broadly tuned odorant receptors to produce specific population codes for different odors. In the olfactory bulb, these receptors are arrayed into a spatial map of glomeruli, such that each odor activates a unique spatial pattern of activity<sup>1–3</sup>. Rats can discriminate odorants with highly overlapping glomerular representations<sup>4,5</sup>, indicating that subtle differences in spatial representations can provide enough information for nearly perfect discrimination. What are the mechanisms that support this fine discrimination? It has been proposed that the glomerular map can provide a mechanism to enhance contrast between similar odors by using lateral inhibition between neighboring neurons in the olfactory bulb<sup>6,7</sup>. The intrinsic dynamical properties of the olfactory system<sup>8–10</sup> have also been proposed to provide temporal coding mechanisms that might facilitate odor discrimination<sup>10–13</sup>. On a fast time scale, stimulus-specific ensembles of neurons synchronize their firing to gamma frequency (30–100 Hz) oscillations<sup>14–17</sup>. On an intermediate time scale, neurons in the mammalian olfactory system time lock to specific phases of the respiratory cycle<sup>18–21</sup>, which follows a theta-frequency (4–8 Hz) rhythm during odor investigation<sup>22</sup>. On a slow time scale, firing patterns evolve over hundreds of milliseconds to seconds during constant stimulus presentation<sup>15,16,23–25</sup>. In the zebrafish, slow temporal evolution enhances the differences in firing patterns produced by similar odors over 0.5–2 s (ref. 24). Olfactory representations could also be elaborated across sniffing cycles<sup>26,27</sup>, with several sniffs being required to form a fully refined olfactory representation for fine discriminations.

While consistent with the conventional notion that olfaction is a slow sense, the idea that slow temporal coding or repetitive sampling can facilitate discrimination has not been tested psychophysically. These mechanisms imply a tradeoff between speed and accuracy of discrimination over the time scale of the temporal evolution of the representation. Although a number of studies suggest that the identifica-

tion of distinct odors can be achieved in  $\leq 0.5$  s (for example, see refs. 28–31), none of these studies considered difficult discriminations of highly similar odors, which may be a prerequisite for the involvement of temporal coding<sup>16,20</sup>. Indeed, reaction times for humans performing relatively difficult binary mixture discriminations are remarkably slow, in the 1–2 s range<sup>32</sup>. Here, we used a psychophysical approach to directly test the speed and accuracy of odor discrimination by rats.

## RESULTS

We trained rats using operant conditioning to perform a two-alternative choice odor discrimination (Fig. 1a,b; see **Supplementary Video** online). Although the odor was available for up to 1 s, all animals used much shorter odor sampling periods. For a dissimilar odor pair (valeric acid versus hexanol), which the rat discriminated at an accuracy of 97.4%, the median odor sampling time (between odor onset and withdrawal from the odor port) was 223 ms, and the median movement time (between withdrawal from the odor port and entry into the choice port) was 274 ms (Fig. 1c). Nearly identical results were obtained with odor pairs with highly overlapping glomerular activation patterns. The same rat discriminated the stereoisomers S(+)-2-octanol and R(-)-2-octanol with median odor sampling and movement times of 229 ms and 272 ms, respectively, at an accuracy of 95.6% (Fig. 1d).

### Discrimination speed is independent of chemical similarity

Using a series of odorants with different structural features, we examined the relationship between similarity in glomerular representations and the accuracy and timing of the discrimination. To quantify similarity of glomerular activation patterns, we used intrinsic optical imaging to map the responses of the olfactory bulb to three aliphatic acids (caproic acid, butyric acid, valeric acid) and four alcohols (heptanol, hexanol and S(+)- and R(-)-2-octanol) (**Supplementary Fig. 1** online). Glomerular activity patterns were more similar within each

Cold Spring Harbor Laboratory, 1 Bungtown Road, Cold Spring Harbor, New York 11724, USA. Correspondence should be addressed to Z.F.M. (zach@cshl.org).

Published online 19 October 2003; doi:10.1038/nn1142

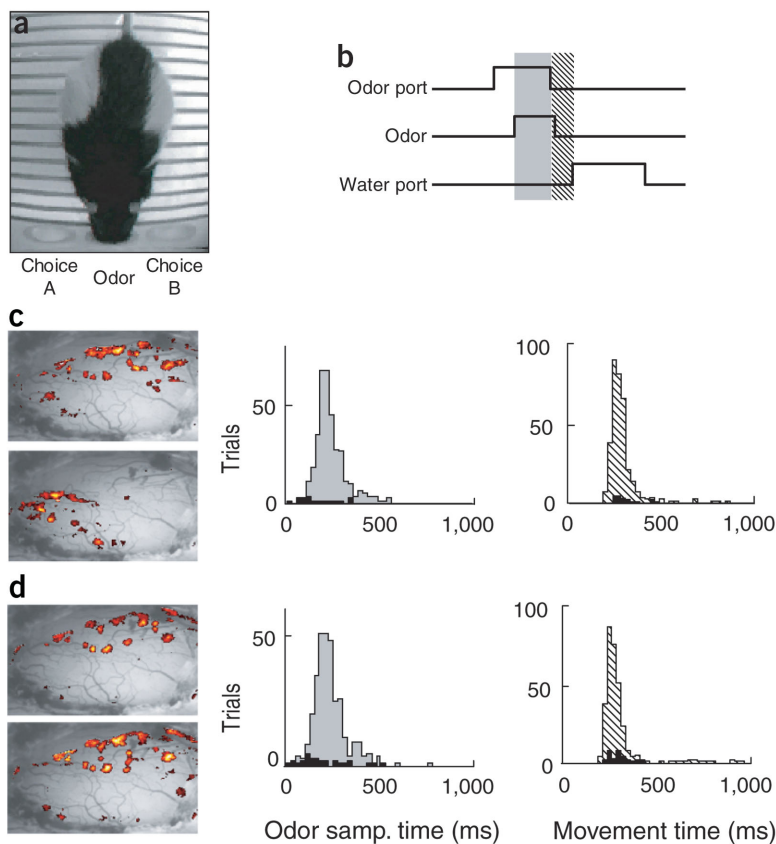


**Figure 1** Rapid odor discrimination in monomolecular discrimination.

(a) Still frame of a rat performing a two-alternative forced-choice odor discrimination task. The rat is shown making a nose poke at the central odor port to trigger the delivery of an odor. Subsequently, the rat is rewarded for making a nose poke at the correct choice port (A or B), depending on the identity of the odor. (b) Diagram of the timing of task events. Nose poke signals were recorded using photodetectors across the sample and water choice ports. The odor sampling time is the latency from odor onset to withdrawal of nose from odor port (gray shading). The movement time is the latency from nose withdrawal from odor port to nose entry into choice port (hatching). (c, d) Distribution of odor sampling (left) and movement time (right) from one rat discriminating a dissimilar odor pair (c, valeric acid versus hexanol) and a similar odor pair (d, S(+)- and R(-)-2-octanol). Gray/hatched histogram bars represent correct trials; black bars represent error trials. Images at left show glomerular activity evoked by the corresponding odors (see **Supplementary Fig. 1** online).

each of these monomolecular odor pairs, yielding a data set of 34,000 trials. Subjects discriminated each pair with >90% accuracy, but there was a significant correlation between odor similarity and accuracy (Fig. 2b;  $R^2 = 0.88$ ,  $P < 0.01$ ;  $n = 4$ ). In contrast, odor sampling time was not significantly correlated with odor similarity (Fig. 2c;  $R^2 = 0.035$ ,  $P > 0.72$ ), and there was no correlation between movement time and odor similarity (Fig. 2d;  $R^2 = 0.56$ ,  $P > 0.05$ ). Thus, the ability of the rat to accurately discriminate odorants activating largely overlapping glomerular representations did not require a sacrifice in speed.

#### Discrimination speed is independent of mixture difficulty

Because these high performance levels might suggest that monomolecular odors are not sufficiently similar to challenge the rat's olfactory

of these two classes than between classes<sup>33</sup>, with the most similar activation patterns obtained with the 2-octanol stereoisomers (Fig. 1c,d). Odor similarity was quantified using a vector distance metric and displayed using a hierarchical clustering method (Fig. 2a).

Based on these glomerular activity patterns, we selected four 'similar' odor pairs (S(+)-2-versus R(-)-2-octanol, hexanol versus heptanol, caproic acid versus valeric acid, and caproic acid versus butyric acid) and two 'dissimilar' odor pairs (caproic acid versus hexanol, valeric acid versus hexanol). Four rats were trained and tested on

**Figure 2** Odor sampling times are independent of odor similarity. (a) Cluster analysis of glomerular activation patterns. The glomerular activation pattern produced by each odorant obtained using intrinsic signal imaging (**Supplementary Fig. 1** online) was treated as a vector, and cluster analysis was performed using a normalized (cosine) distance metric, which ranges from 0 (identical vectors) to 1 (orthogonal vectors) (see **Supplementary Methods** online). Note that odorants with the same functional group produced more similar activation patterns than those with different functional groups. (b-d) Performance accuracy (b), odor sampling time (c) and movement time (d) are plotted as a function of dissimilarity in glomerular representation. Each point contains data from one of six pure odor pairs presented interleaved with eight total mixtures. In all panels,  $n = 5$  rats for imaging experiments,  $n = 4$  rats for behavioral measurements. Note that error bars are smaller than symbols in most cases.

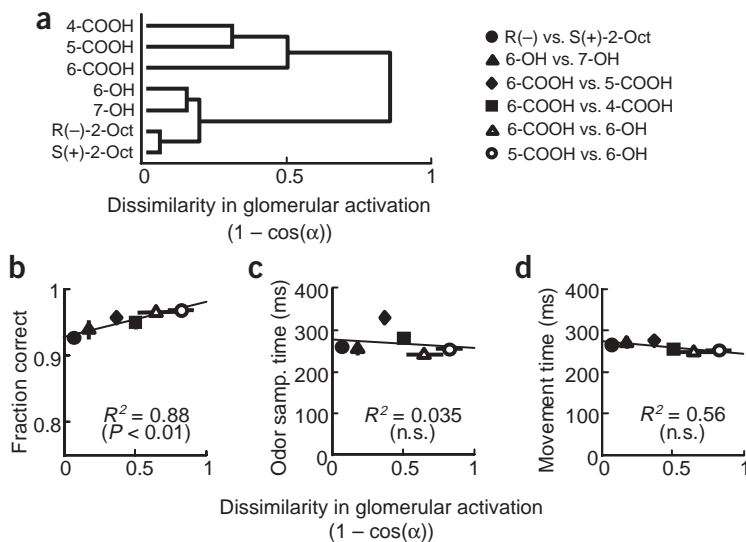
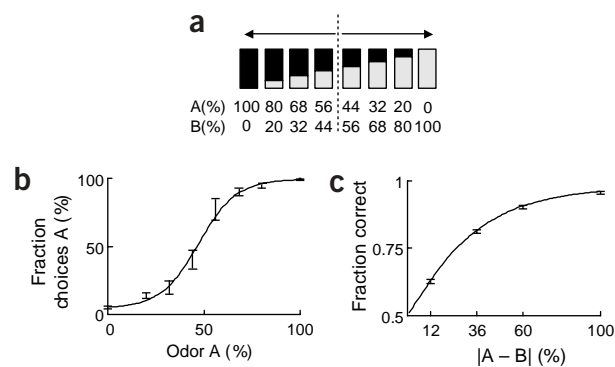


**Figure 3** Parametric manipulation of odor quality and discrimination difficulty using a binary odor mixture discrimination task. (a) Mixture discrimination task stimuli and reward contingencies. Two odorants (A and B) were mixed in eight different ratios, and the rat was rewarded for choosing the odor associated with the dominant odorant of the mixture. (b) Performance of one rat in discriminating valeric acid and hexanol (same rat as Fig. 1c,d). Data from ten sessions (176–288 trials/session) were fitted using a logistic function. (c) Discrimination accuracy as a function of mixture ratio ( $n = 4$  rats). Each pair of corresponding mixture ratios was pooled (0/100 and 100/0, etc.) and plotted as the absolute value of the difference of the pair (e.g.,  $|80 - 20| = |20 - 80| = 60$ ). A cumulative Weibull function was fitted using a maximum-likelihood algorithm<sup>47</sup>.



system, we increased the difficulty of each odor discrimination by requiring the subjects to discriminate mixtures containing different proportions of two odors (Fig. 3a). For each odor pair, eight different interleaved mixture ratios were used, and choices were rewarded according to the dominant component of the mixture (Fig. 3a). This procedure yielded sigmoidal psychometric performance functions (Fig. 3b), with discrimination accuracy dropping sharply for mixture ratios near 50/50 (Fig. 3c).

Even pushing discrimination capabilities toward their psychophysical limits using these much more difficult binary mixtures did not result in a significant change in the speed of discrimination. Odor sampling increased by <35 ms as accuracy dropped from 90–95% for pure odors to 60–65% for the most difficult mixtures ( $P < 0.01$ , Friedman's two-way ANOVA; Fig. 4a). Movement times did not vary across any condition ( $P > 0.09$ ; Fig. 4b).

To further test whether rapid odor discrimination behavior holds in different experimental conditions, we tested the effects of (i) delivering single difficult mixture pairs throughout a session, (ii) lowering the odor concentration 100-fold and (iii) increasing the variance of the random foreperiod (latency between nose poke and odor onset) (Supplementary Fig. 2 online). None of these manipulations increased the absolute odor sampling time or the dependence of odor sampling time on discrimination difficulty. Thus, rats adopt a rapid odor sampling strategy for discrimination that is not only independent of the difficulty of the problem, but is also insensitive to important task parameters.

#### Discrimination accuracy saturates after short odor sampling time

Next, to examine the dependence of accuracy on sampling time independent of task manipulations, we used a conditional accuracy analysis<sup>34</sup>, which makes use of the natural variability in reaction time within a single condition. For each odor pair and mixture ratio, we partitioned trials according to odor sampling time to produce a conditional accuracy function (Fig. 5a). Discrimination accuracy increased over the first 200 ms, but then flattened regardless of the mixture ratio. The odor sampling time distribution was well-matched to the shape of the conditional accuracy function, with the bulk of the

odor sampling times corresponding to latencies shortly after accuracy peaked (histogram in Fig. 5a). The latency-to-peak accuracy did not increase with the difficulty of the odor mixture ( $P > 0.9$ , Friedman's two-way ANOVA; Fig. 5b). Furthermore, performance was either uncorrelated or negatively correlated with odor sampling time beyond 250 ms in 95 out of 96 experimental conditions (Spearman's rank correlation coefficient). Thus, beyond a relatively short minimum, longer odor sampling times tended to be associated with degraded rather than improved accuracy (Fig. 5c,d).

#### Maximum discrimination accuracy is achieved in one sniff

The brevity of the odor sampling period necessary to reach accurate discriminations suggests that maximum performance may be achieved in one odor sample—a single sniff. To measure the sniffing pattern underlying odor sampling directly, three rats were implanted with temperature sensors to measure nasal airflow (Fig. 6a). An approximately linear relationship between the number of sniffs and the odor sampling duration was observed, with a mean sniffing frequency of  $7.5 \pm 1.6$  Hz ( $n = 3$ ), corresponding to theta frequency<sup>22</sup>. Sniffing frequency was highest at odor onset and declined slightly during the odor sampling period (Fig. 6b). By counting individual inhalations, we obtained a more exact count of the number of sniffs on each trial. Rats usually took one or two sniffs to discriminate (median  $1.96 \pm 0.61$  sniffs), and there was no change in the number of sniffs with difficulty (Fig. 6c). When trials were partitioned according to the number of sniffs, analogous to the conditional accuracy function, it could be seen that discrimination accuracy reached an asymptote in just one sniff (Fig. 6d). Trials with less than one full inhalation (odor onset occurring during the inhalation) resulted in poor performance, but there was <5% difference in accuracy between trials of one and two sniffs regardless of the difficulty of the mixture discrimination. Thus, repetitive sampling did not result in a substantial improvement in odor discrimination.

#### DISCUSSION

We used graded odor mixtures in a two-alternative forced-choice task to produce a psychophysical paradigm in which quality and difficulty could be parametrically varied to yield regular psychometric functions<sup>35</sup>. Reaction time measurements in similar two-alternative choice tasks have long been used in human psychophysics to constrain models of decision-making<sup>34</sup>. In contrast to many human decision-making studies, we found very little tradeoff between the

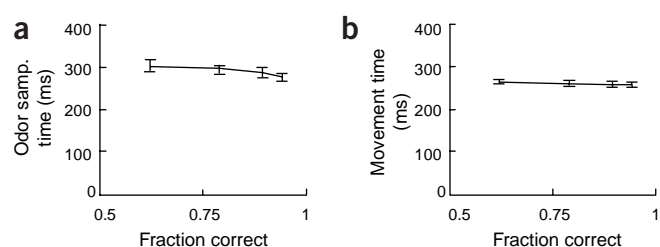


**Figure 4** Odor sampling times are fast and largely independent of discrimination difficulty. (a,b) Median odor sampling time (a) and movement time (b) as a function of choice accuracy. Each point represents a single mixture ratio pooled across six odor pairs.

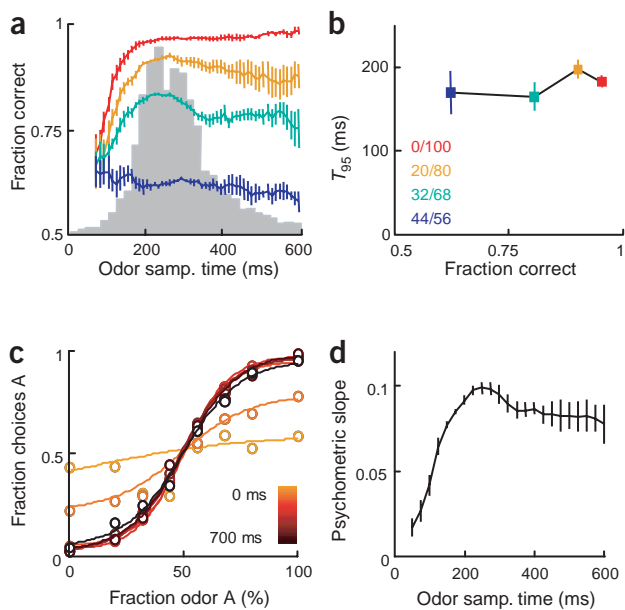


**Figure 5** Odor discrimination accuracy shows asymptotic curve after brief odor sampling time. (a) Accuracy as a function of odor sampling time (conditional accuracy function<sup>34</sup>). Colors correspond to mixture ratios as indicated in b. The distribution of odor sampling times is shown in the background ( $n = 4$  rats, 6 odors). (b) The time to reach 95% of asymptotic accuracy ( $T_{95}$ ) for all odor pairs. Colors correspond to mixture ratios as indicated. (c) Trials were partitioned by odor sampling time in 100-ms bins, and a logistic function was fitted to each psychometric function. (d) The slopes of the fitted psychometric functions are plotted as a function of odor sampling time. Note that discriminability decreased with odor sampling time after 200 ms. In all panels, data was pooled across all six odor pairs.

mechanisms such as synchrony<sup>13–17</sup> or rank-order<sup>36</sup> coding could also provide suitably rapid olfactory representations.

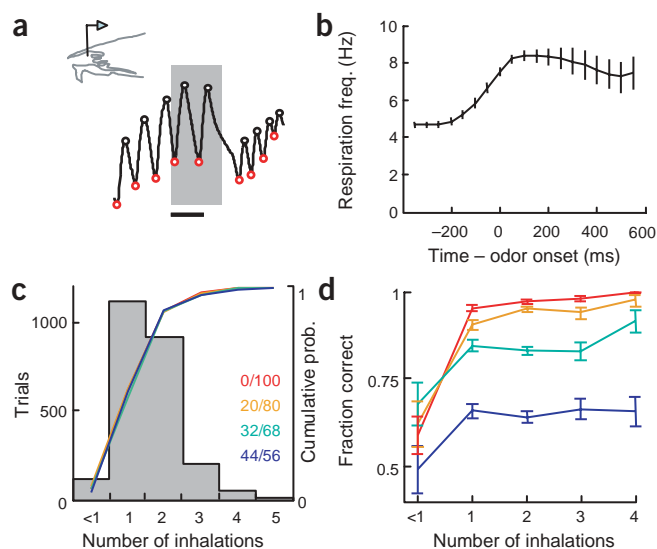
We found no evidence that rats used repeated samples to form a more refined representation of odor identity. Mechanistically, this suggests that olfactory information may be temporally chunked or quantized by the respiration cycle, such that each sniff constitutes a discrete olfactory sensory image, or snapshot. In mammals, the motor act of sniffing is tightly coupled to the perceptual process of olfaction<sup>37</sup>. In species that do not sniff, analogous motor rhythms drive stimuli over olfactory receptors, including antennal flicking in arthropods<sup>38</sup>, casting through odor plumes in moths<sup>39</sup> and coughing in fish<sup>40</sup>. The respiration cycle may be crucial to the encoding of olfactory sensory information. The firing of olfactory neurons is strongly patterned by the respiratory rhythm, and information about odor identity and concentration can be encoded in the phase of spiking relative to respiration-driven oscillations<sup>18,20,21,41,42</sup>. The respiration cycle may also be important to the integration of olfactory sensory information with cognitive and motor processes. Theta-frequency local field potentials in the hippocampus show selective phase relationships to the respiration cycle<sup>43</sup>. Theta-frequency synchrony may simplify the process of sensorimotor integration by imposing more strict temporal relationships among activity across brain regions.

Although discrimination might in principle benefit from more extensive temporal integration, the advantages of rapid and discrete odor images may outweigh the limitations. For example, the accuracy of concentration estimation could be enhanced by resetting accumulated information with each sniff, helping to localize odor sources through concentration gradients. Limiting temporal integration

difficulty of discrimination and the required odor sampling time. Regardless of odor similarity, rats sampled only briefly, taking ~300 ms or about two sniffs to perform a discrimination. Analysis using natural variability in the odor sampling period showed that maximum accuracy was achieved in less than 200 ms, corresponding to just one sniff. Although more sniffs are often taken, discrimination accuracy did not improve with this extended sampling. Thus, the discrimination of even two subtly different blends of structurally similar chemicals, activating largely overlapping glomerular representations, can be carried out as fast as the limits imposed by the olfactory sampling process.

These results place stringent constraints on the time scale over which neural activity must evolve in order to render accurate olfactory perceptual discriminations. Performance of fine odor discriminations by the rat does not depend on slow temporal processing, as this would have introduced an obligatory increase in accuracy during the refinement of the representation. Although temporal patterns of neural activity may take hundreds of milliseconds or even seconds to evolve<sup>14,15,24,25</sup>, any temporal decorrelation that is necessary for disambiguation of overlapping spatial patterns for a binary odor discrimination appears to develop over the time scale of tens of milliseconds rather than hundreds or thousands. Fast neural coding

**Figure 6** Peak discrimination accuracy requires one sniff, regardless of difficulty. (a) Example trace of the respiratory signal. Red circles, onset of inhalation; black circles, onset of exhalation. The inset diagram shows the placement of the thermocouple in a sagittal section through the nose. The gray shading is the odor sampling period (time from odor onset to nose poke withdrawal). Scale bar, 250 ms. (b) Respiration (sniffing) frequency during odor sampling ( $n = 3$  rats). Note the elevation in frequency during odor sampling and slight decline with odor sampling time. Only inhalations occurring before nose poke withdrawal were included. Graphs in b and d show the same data set (3 rats; 7,085 trials, 71 sessions; caproic acid versus hexanol). (c) Distribution of the number of sniffs during the odor sampling period for a single rat pooled across all trials (gray shading). Cumulative distribution functions for the number of sniffs are shown separated by mixture ratios. The category “<1” contains trials with no inhalation or in which odor onset occurred during an inhalation. (d) Choice accuracy as a function of number of sniffs. Line colors correspond to mixture ratios as indicated in c.



would also enhance the precision with which specific odor images could be mapped to specific locations, helping to build a more detailed map of an olfactory environment.

Discrimination is crucial to making differential responses to stimuli according to their significance. Since the present study focused on well-trained animals, it will be interesting to determine whether learning or categorizing a novel odor requires additional computations and processing time. In natural environments, animals also face more complex problems such as concentration- and background-invariant odor recognition and odor source localization<sup>44</sup>. The use of appropriate psychophysical paradigms will be critical to understanding the full complexity of neural coding in the olfactory system.

## METHODS

All procedures involving animals were carried out in accordance with National Institutes of Health standards as approved by the Cold Spring Harbor Laboratory Institutional Animal Care and Use Committee. All statistics are mean  $\pm$  standard error of the mean (s.e.m.) unless otherwise noted. Detailed methods can be found in **Supplementary Methods** online.

**Odor discrimination task.** Male Long-Evans hooded rats were tested in behavioral experiments using water restriction for motivation. Performance was monitored, and delivery of odors and water reinforcement were controlled using computer data acquisition hardware (National Instruments) and custom software written in Matlab (Mathworks). Subjects initiated trials by a nose poke into the odor sampling port, which triggered the delivery of an odor for up to 1 s. Reward was available for correct choices for up to 2 s after the rat left the odor sampling port. The training and testing conditions emphasized accuracy over speed. In particular, a minimum inter-trial interval of 4 s from the choice poke to the start of the next valid trial was imposed, so even a relatively large fractional increase in the duration of odor sampling time would have a small impact on the time to the next trial. Odor sampling times were characterized using the median and include correct trials only. In all cases, the results reported were unchanged by the inclusion of error trials.

**Odor delivery.** Odors were delivered using a custom-made olfactometer (**Supplementary Fig. 3** online). Binary odor mixtures in eight proportions (100/0, 80/20, 68/32, 56/44, 44/56, 32/68, 20/80 and 0/100) were delivered in pseudorandom order within a session, except where noted. The mixture ratios were produced by differential air flow dilution using a pair of mass flow controllers. To measure the latency of odor arrival at the nose, we recorded the odor-evoked electro-olfactogram (EOG) in four urethane-anesthetized rats. To allow for a possible delay in the EOG relative to odor reaching the epithelium, we subtracted a latency of 32 ms (ref. 45) to obtain a more conservative estimate, which was used for all calculations of odor sampling time.

**Intrinsic signal imaging.** To quantify the similarity of glomerular activity evoked by different pairs of odorants, standard methods were used to image intrinsic signals in the dorsal olfactory bulb. High-pass spatial filtering was used to help identify punctate (presumably glomerular) signals<sup>46</sup>, and an array of signal intensity values was extracted for each odor using small regions of interest placed over these puncta (**Supplementary Fig. 4** online). Odor similarity was calculated using a normalized distance metric and displayed using a hierarchical clustering analysis (**Supplementary Fig. 5** online).

*Note: Supplementary information is available on the Nature Neuroscience website.*

## ACKNOWLEDGMENTS

We thank S. Edgar, H. Zariwala, E. Friedman and G. Agarwal for behavioral training and testing, and R. Gasperini for development of instruments. We thank members of our group and colleagues at CSHL for discussion, as well as T. Zador, C. Brody, R. Malinow, A. Kepecs, M. DeWeese, M. Tanifuji and Y. Yoshihara for comments on a previous version of the manuscript. Supported by the National Institute on Deafness and Other Communication Disorders (5R01DC006104-02), Searle Scholars Program, Packard Foundation and Burroughs Wellcome Fund (Z.F.M.), as well as by a fellowship from the Japan Society for the Promotion of Science and the Cold Spring Harbor Laboratory Association (N.U.).

## COMPETING INTERESTS STATEMENT

The authors declare that they have no competing financial interests.

Received 6 August; accepted 24 September 2003

Published online at <http://www.nature.com/natureneuroscience/>

- Korsching, S.I. Odor maps in the brain: spatial aspects of odor representation in sensory surface and olfactory bulb. *Cell. Mol. Life Sci.* **58**, 520–530 (2001).
- Leon, M. & Johnson, B.A. Olfactory coding in the mammalian olfactory bulb. *Brain Res. Brain Res. Rev.* **42**, 23–32 (2003).
- Mori, K. Grouping of odorant receptors: odour maps in the mammalian olfactory bulb. *Biochem. Soc. Trans.* **31**, 134–136 (2003).
- Rubin, B.D. & Katz, L.C. Spatial coding of enantiomers in the rat olfactory bulb. *Nat. Neurosci.* **4**, 355–356 (2001).
- Linster, C., Johnson, B.A., Morse, A., Yue, E. & Leon, M. Spontaneous versus reinforced olfactory discriminations. *J. Neurosci.* **22**, 6842–6845 (2002).
- Yokoi, M., Mori, K. & Nakanishi, S. Refinement of odor molecule tuning by dendrodendritic synaptic inhibition in the olfactory bulb. *Proc. Natl. Acad. Sci. USA* **92**, 3371–3375 (1995).
- Mori, K., Nagao, H. & Yoshihara, Y. The olfactory bulb: coding and processing of odor molecule information. *Science* **286**, 711–715 (1999).
- Adrian, E.D. The electrical activity of the mammalian olfactory bulb. Electroencephalography. *Clin. Neurophysiol.* **2**, 377–388 (1950).
- Gelperin, A. & Tank, D.W. Odour-modulated collective network oscillations of olfactory interneurons in a terrestrial mollusc. *Nature* **345**, 437–440 (1990).
- Freeman, W.J., Skarda, C.A. How brains make chaos in order to make sense of the world. *Behav. Brain Sci.* **10**, 161–195 (1987).
- Laurent, G. Olfactory network dynamics and the coding of multidimensional signals. *Nat. Rev. Neurosci.* **3**, 884–895 (2002).
- Rabinovich, M. *et al.* Dynamical encoding by networks of competing neuron groups: winnerless competition. *Phys. Rev. Lett.* **87**, 068102 (e-pub, 2001).
- Brody, C.D. & Hopfield, J.J. Simple networks for spike-timing-based computation, with application to olfactory processing. *Neuron* **37**, 843–852 (2003).
- Laurent, G. & Davidowitz, H. Encoding of olfactory information with oscillating neural assemblies. *Science* **265**, 1872–1875 (1994).
- Wehr, M. & Laurent, G. Odour encoding by temporal sequences of firing in oscillating neural assemblies. *Nature* **384**, 162–166 (1996).
- Stopfer, M., Bhagavan, S., Smith, B.H. & Laurent, G. Impaired odour discrimination on desynchronization of odour-encoding neural assemblies. *Nature* **390**, 70–74 (1997).
- Kashiwadani, H., Sasaki, Y.F., Uchida, N. & Mori, K. Synchronized oscillatory discharges of mitral/tufted cells with different molecular receptive ranges in the rabbit olfactory bulb. *J. Neurophysiol.* **82**, 1786–1792 (1999).
- Macrides, F. & Chorover, S.L. Olfactory bulb units: activity correlated with inhalation cycles and odor quality. *Science* **175**, 84–87 (1972).
- Chaput, M.A. EOG responses in anesthetized freely breathing rats. *Chem. Senses* **25**, 695–701 (2000).
- Margrie, T.W. & Schaefer, A.T. Theta oscillation coupled spike latencies yield computational vigour in a mammalian sensory system. *J. Physiol.* **546**, 363–374 (2003).
- Cang, J. & Isaacson, J.S. *In vivo* whole-cell recording of odor-evoked synaptic transmission in the rat olfactory bulb. *J. Neurosci.* **23**, 4108–4116 (2003).
- Welker, W.I. Analysis of sniffing of the albino rat. *Behavior* **22**, 223–244 (1964).
- Laurent, G. & Naraghi, M. Odorant-induced oscillations in the mushroom bodies of the locust. *J. Neurosci.* **14**, 2993–3004 (1994).
- Friedrich, R.W. & Laurent, G. Dynamic optimization of odor representations by slow temporal patterning of mitral cell activity. *Science* **291**, 889–894 (2001).
- Meredith, M. Patterned response to odor in mammalian olfactory bulb: the influence of intensity. *J. Neurophysiol.* **56**, 572–597 (1986).
- Stopfer, M. & Laurent, G. Short-term memory in olfactory network dynamics. *Nature* **402**, 664–668 (1999).
- Ambros-Ingerson, J., Granger, R. & Lynch, G. Simulation of paleocortex performs hierarchical clustering. *Science* **247**, 1344–1348 (1990).
- Karpov, A.P. Analysis of neuron activity in the rabbit's olfactory bulb during food-acquisition behavior in *Neural Mechanisms of Goal-directed Behavior* (eds. Thompson, R.F., Hicks, L.H. & Shyrkov, V.B.) 273–282 (Academic, New York, 1980).
- Laing, D.G. Identification of single dissimilar odors is achieved by humans with a single sniff. *Physiol. Behav.* **37**, 163–170 (1986).
- Goldberg, S.J. & Moulton, D.G. Olfactory bulb responses telemetered during an odor discrimination task in rats. *Exp. Neurol.* **96**, 430–442 (1987).
- Slotnick, B. M. Olfactory perception in *Comparative Perception* (eds. Stebbins, W. & Berkley, M.) 155–244 (Wiley, New York, 1990).
- Wise, P.M. & Cain, W.S. Latency and accuracy of discriminations of odor quality between binary mixtures and their components. *Chem. Senses* **25**, 247–265 (2000).
- Uchida, N., Takahashi, Y.K., Tanifuji, M. & Mori, K. Odor maps in the mammalian olfactory bulb: domain organization and odorant structural features. *Nat. Neurosci.* **3**, 1035–1043 (2000).
- Luce, R.D. *Response Times: Their Role in Inferring Elementary Mental Organization* (Oxford Univ. Press, New York, 1986).

35. Parker, A.J. & Newsome, W.T. Sense and the single neuron: probing the physiology of perception. *Annu. Rev. Neurosci.* **21**, 227–277 (1998).
36. VanRullen, R. & Thorpe, S.J. The time course of visual processing: from early perception to decision-making. *J. Cogn. Neurosci.* **13**, 454–461 (2001).
37. Johnson, B.N., Mainland, J.D. & Sobel, N. Rapid olfactory processing implicates subcortical control of an olfactomotor system. *J. Neurophysiol.* **90**, 1084–1094 (2003).
38. Atema, J. Chemical signals in the marine environment: dispersal, detection, and temporal signal analysis. *Proc. Natl. Acad. Sci. USA* **92**, 62–66 (1995).
39. Vickers, N.J. & Baker, T.C. Reiterative responses to single strands of odor promote sustained upwind flight and odor source location by moths. *Proc. Natl. Acad. Sci. USA* **91**, 5756–5760 (1994).
40. Nevitt, G.A. Do fish sniff? A new mechanism of olfactory sampling in pleuronectid flounders. *J. Exp. Biol.* **157**, 1–18 (1991).
41. Chaput, M. A. Respiratory-phase-related coding of olfactory information in the olfactory bulb of awake freely-breathing rabbits. *Physiol. Behav.* **36**, 319–324 (1986).
42. Spors, H. & Grinvald, A. Spatio-temporal dynamics of odor representations in the mammalian olfactory bulb. *Neuron* **34**, 301–315 (2002).
43. Macrides, F., Eichenbaum, H.B. & Forbes, W.B. Temporal relationship between sniffing and the limbic theta rhythm during odor discrimination reversal learning. *J. Neurosci.* **2**, 1705–1717 (1982).
44. Hopfield, J.J. Odor space and olfactory processing: collective algorithms and neural implementation. *Proc. Natl. Acad. Sci. USA* **96**, 12506–12511 (1999).
45. Mackay-Sim, A. & Kesteven, S. Topographic patterns of responsiveness to odorants in the rat olfactory epithelium. *J. Neurophysiol.* **71**, 150–160 (1994).
46. Meister, M. & Bonhoeffer, T. Tuning and topography in an odor map on the rat olfactory bulb. *J. Neurosci.* **21**, 1351–1360 (2001).
47. Wichmann, F.A. & Hill, N.J. The psychometric function: fitting, sampling, and goodness of fit. *Percept. Psychophys.* **63**, 1293–1313 (2001).